

Coordination chemistry of an amine-substituted bis(pyrazolyl)-pyridine ligand: interaction of a peripheral functional group on a coordination cage with the internal contents of the cavity

Alexander J. Metherell & Michael D. Ward

To cite this article: Alexander J. Metherell & Michael D. Ward (2017): Coordination chemistry of an amine-substituted bis(pyrazolyl)-pyridine ligand: interaction of a peripheral functional group on a coordination cage with the internal contents of the cavity, *Supramolecular Chemistry*, DOI: [10.1080/10610278.2017.1388509](https://doi.org/10.1080/10610278.2017.1388509)

To link to this article: <http://dx.doi.org/10.1080/10610278.2017.1388509>



Published online: 12 Oct 2017.



Submit your article to this journal [↗](#)



Article views: 4



View related articles [↗](#)



View Crossmark data [↗](#)



Coordination chemistry of an amine-substituted bis(pyrazolyl)-pyridine ligand: interaction of a peripheral functional group on a coordination cage with the internal contents of the cavity

Alexander J. Metherell  and Michael D. Ward 

Department of Chemistry, University of Sheffield, Sheffield, UK

ABSTRACT

The ligand L^{an} contains two bidentate chelating pyrazolyl-pyridine termini connected to a central aminophenyl ring. In $[Ag_3(L^{an})_2](ClO_4)_3$ each ligand coordinates in a pentadentate 2+1+2 manner, connecting all three Ag(I) ions. In contrast, in the octanuclear cubic coordination cage $[Co_8(L^{an})_{12}][BF_4]_{16}$ each L^{an} coordinates as a bis(pyrazolyl-pyridine) tetradentate chelate, with the externally-directed amine groups not coordinated. From its 1H NMR spectrum this cage has the S_6 symmetric structure containing two *fac* and six *mer* tris-chelate Co(II) centres of other octanuclear cages. Slow crystallisation afforded $[Co_8(L^{an})_{12}Na][BF_4]_{17}$, with S_4 symmetry arising from four *fac* and four *mer* tris-chelate Co(II) centres which alternate; the central cavity accommodates an Na^+ cation and four fluoroborate anions which form a $\{Na(BF_4)_4\}^{3-}$ guest. The $\{Na(BF_4)_4\}^{3-}$ guest forms $F\cdots HN$ hydrogen bonds through the cage windows with exterior amine groups. Rearrangement of the cage structure from S_6 to S_4 symmetry appears to facilitate inclusion of the fourfold symmetric guest.

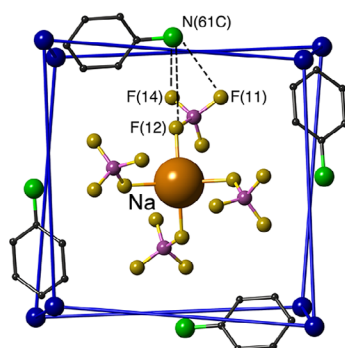
ARTICLE HISTORY

Received 25 July 2017

Accepted 29 September 2017

KEYWORDS

Polydentate ligand;
coordination cage; host-guest chemistry



Introduction

In the well-established field of self-assembled coordination cages (1), the focus of many research groups has shifted from synthesis (through design or serendipitous discovery of new cage structures) to the development of useful functions of cage molecules associated with binding of guests in the central cavity (2). Such work has afforded diverse functions from drug transport and delivery (3) to catalysed reactions of bound guests, and in most cases is based on reversible uptake/release of guests and the altered microenvironment within the cage cavity.

In some cases however modification of cages by addition of either externally-directed or inwardly-directed functional groups provides more sophisticated possibilities

for the introduction of functional behaviour. For example, the Fujita group has prepared a series of ligands based on a 1,3-bis(4-pyridyl)benzene backbone which are the basis of a series of approximately spherical $Pd_{12}L_{24}$ cage complexes. Substitution at the 5-position of the phenylene spacer allows the formation of a series of $M_{12}L_{24}$ cages which have 24 pendant substituents decorating the exterior surface of the cage; this is an example of *exohedral* functionalization (4). These substituents (including metallo-porphyrins, saccharides, DNA strands and hexapeptide aptamers) contribute to strong and selective interactions of the spherical complexes with a wide variety of substrates, which do not occur when the unfunctionalised ligand is used; for example, the saccharide coated molecular sphere forms aggregates with the

protein concanavalin A (5). The same group has also used a series of ligands which are substituted at the 2-position of the phenyl spacer (i.e. the concave position, internally-directed) of an elongated ligand, such that the resulting $M_{12}L_{24}$ cages contain 24 inwardly directed substituents, which are examples of *endohedral* functionalization (6). This has (for example) allowed the formation of precisely monodisperse silica nanoparticles within the cage cavity lined with 24 inwardly directed sugar groups (7).

In a similar vein, other examples of endohedral functionalization of cage complexes include attachment of BODIPY fluorophores, from the Nitschke group (8); urea-based hydrogen-bond donor sites, which facilitate strong binding of oxoanion guests, from Custelcean and co-workers (9); and amine-based hydrogen-bond donors, which facilitate binding of anionic guests, from Amouri and co-workers (10). Examples of exohedral functionalization include Crowley's attachment of luminescent units to dinuclear Pd_2L_4 cages (11), and our own attachment of 24 hydroxymethyl groups to the external surface of M_8L_{12} cubic cages to help render them water-soluble (12), which allowed access to extensive host-guest chemistry based on the hydrophobic effect (13).

In this paper we report studies into the preparation and coordination behaviour of ligands based on inclusion of an aniline unit as a spacer between the two bidentate pyrazolyl-pyridine chelating units that we customarily employ. The aim is to provide a handle for exohedral functionalization of members of our cage family which may allow (i)

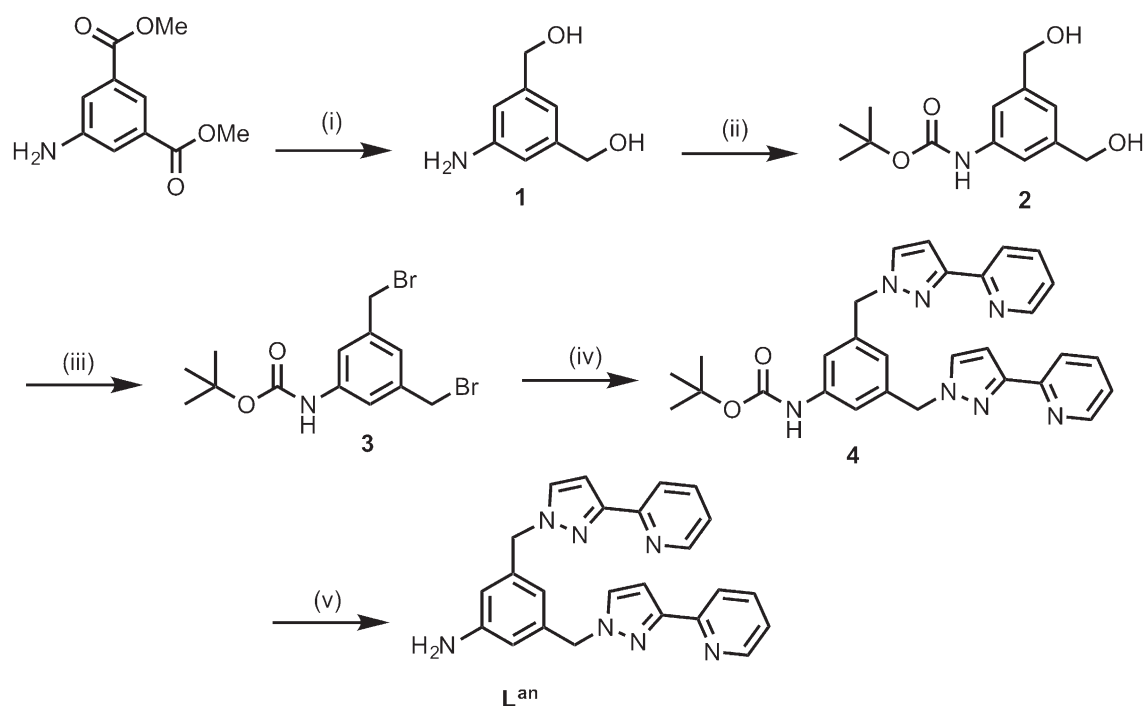
attachment of units with useful functional behaviour to the external surface of the cage, and/or (ii) control of solubility – an important issue given the solvent-dependence of guest binding (13).

Results and discussion

Ligand synthesis

Synthesis of the ligand L^{an} was achieved in five steps starting from the readily available starting material dimethyl 5-aminoisophthalate (see Scheme 1), and followed a similar synthetic route to that used in a previous communication (14). The di-ester starting material was reduced to the di-alcohol **1** by treatment with excess $LiAlH_4$ in tetrahydrofuran (THF) (15), and subsequently *N*-protected as the carbamate **2** (16). Conversion of the hydroxymethyl to bromomethyl groups of the di-alkyl bromide **3** by an Appel bromination was achieved in good yield following a literature procedure (16); subsequent reaction with 3-(2-pyridyl)-pyrazole in THF/aqueous NaOH afforded **4**. Finally the *tert*-butyl-oxycarbonyl (Boc) protecting group was then removed with trifluoroacetic acid (TFA) in CH_2Cl_2 to give the desired ligand L^{an} .

Slow evaporation of a solution of L^{an} in ethyl acetate and hexane resulted in the formation of crystals of X-ray quality; the crystal structure is shown in Figure 1. The structure displays a transoid arrangement of the two near-planar rings in each pyrazolyl-pyridine fragment.



Scheme 1. Reaction scheme for the preparation of L^{an} . (i) $LiAlH_4$, THF; then H_2O , KOH, EtOAc. (ii) Boc_2O , THF. (iii) CBr_4 , PPh_3 , CH_2Cl_2 . (iv) $PyPzH$, THF, $NaOH_{(aq)}$. (v) TFA, CH_2Cl_2 .

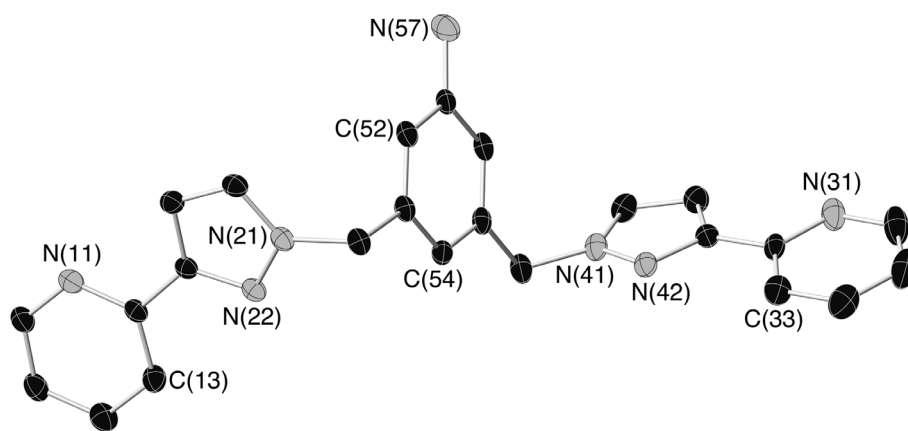


Figure 1. Crystal structure of the ligand $L^{an} \cdot 2.25(H_2O)$ with thermal ellipsoids of non-hydrogen atoms shown at 30% probability.

There are hydrogen bonding interactions between the lattice water molecules and one of the pyrazolyl N atoms [N(22)···O(15) non-bonded separation, 2.88 Å], and also two hydrogen bonds between the aniline group and the pyridyl N atoms of two adjacent molecules [N(57)···N(11), 3.09 Å; N(57)···N(31), 3.24 Å].

Coordination chemistry of L^{an}

Previously we have reported the structurally related ligands L^{m-Ph} and $L^{2,6-Py}$ (Figure 2), both containing a *meta* substituted aromatic ring as the central spacer (17–20). These ligands form a range of structures when mixed with perchlorate or tetrafluoroborate M(II) salts (where M = Co, Ni or Zn), including M_4L_6 squares and M_6L_9 ‘open-books’; but both ligands form an M_8L_{12} cubic cage structure when combined with $Co(BF_4)_2$. It might be expected that similar complexes form when the structurally similar ligand L^{an} is combined with the same metal salts. Accordingly we examined the coordination behaviour of L^{an} with Co(II), and also with Ag(I) given the plasticity of the Ag(I) coordination sphere which optimises the chance of metal/ligand assemblies forming (21).

The reaction between $Ag(ClO_4)$ and L^{an} in a 1:1 ratio in MeOH/ CH_2Cl_2 at room temperature was investigated first. The 1H NMR spectrum of the solid product showed that the ligand has lost its twofold symmetry, with the two pyrazolyl-pyridine termini clearly being inequivalent: for example one of the methylene spacer groups has become diastereotopic, presenting two doublets (at 4.31 and 5.14 ppm) in the 1H NMR spectrum. The crystal structure (Figure 3) reveals the reason for this, with the complex having the formulation $[Ag_3(L^{an})_2](ClO_4)_3$ in which the ligands clearly adopt a non-symmetrical coordination mode.

The structure is of a trinuclear Ag(I) complex forming an approximately isosceles triangle. There are two crystallographically independent but structurally similar complex

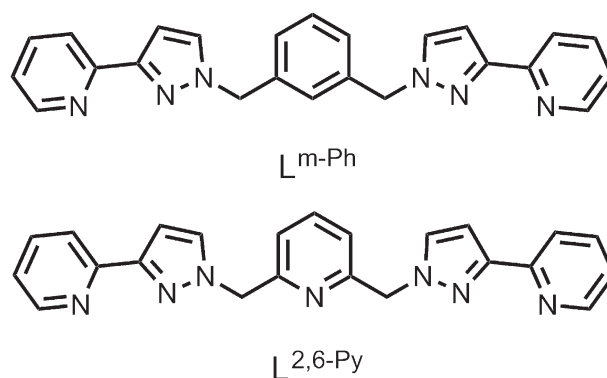


Figure 2. Ligands with a structural similarity to L^{an} that are known to form octanuclear $[Co_8L_{12}](BF_4)_{16}$ cubic coordination cages.

molecules in the asymmetric unit. We describe here the details of the complex containing Ag(1) – Ag(3); structural parameters for the complex molecule based on Ag(4) – Ag(6) are included in Table 1. The two ‘long’ Ag···Ag separations are 9.34 and 9.40 Å [Ag(1)···Ag(2) and Ag(1)···Ag(3), respectively]; the shorter Ag(2)···Ag(3) separation is 5.55 Å. The two ligands (A and B) adopt a trinucleating coordination mode in which one pyrazolyl-pyridine chelate is coordinated to Ag(1) in both cases. In ligand A the amine group of the central spacer (atom N57A) is coordinated to Ag(3), and the second pyrazolyl-pyridine chelate is coordinated to Ag(2); whereas in ligand B the central amine coordinates to Ag(2) and the second pyrazolyl-pyridine to Ag(3). The result is a double helicate arrangement of ligands which are twisted around each other, with both being ‘anchored’ at Ag(1) but having their opposite ends divergent and coordinated to either Ag(2) or Ag(3). This is emphasised in the space-filling view of Figure 4. The two central phenyl rings are approximately parallel to one another and overlapping although the separation between them (>3.7 Å) is slightly longer than ideal for a strong π -stacking interaction.

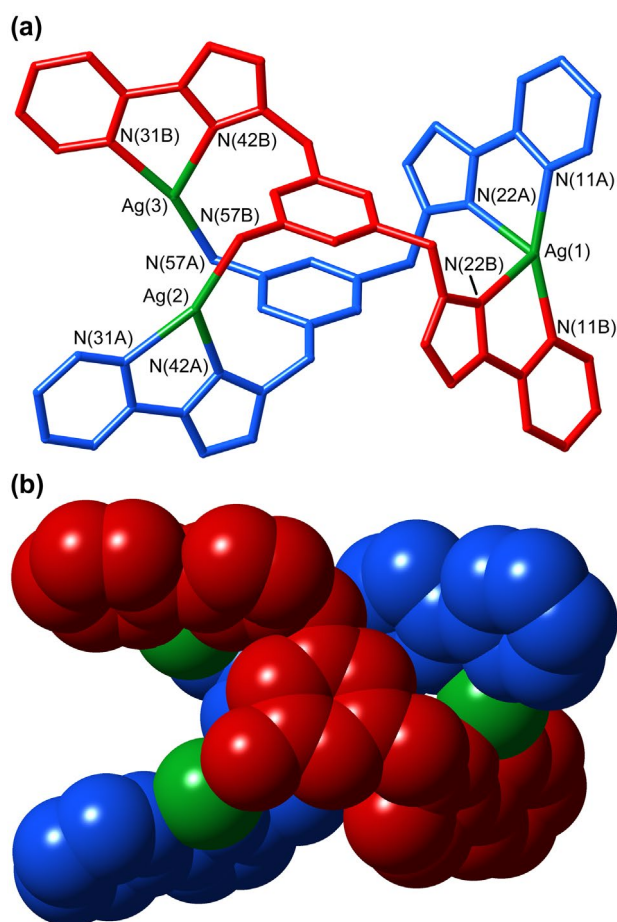


Figure 3. (colour online) Structure of the complex cation of $[\text{Ag}_3(\text{L}^{\text{an}})_2](\text{ClO}_4)_3$, with the two ligands coloured separately for clarity. (a) A view showing the labelling scheme; (b) a space-filling view in the same orientation.

Note: There are two similar but crystallographically independent complexes in the asymmetric unit, with the second one containing Ag(4)/Ag(5)/Ag(6) (see Table 1).

Table 1. Bond distances (Å) and angles ($^\circ$) around the metal ions in the structure of for the structure $[\text{Ag}_3(\text{L}^{\text{an}})_2](\text{ClO}_4)_3 \cdot \text{EtOAc} \cdot \text{MeNO}_2$.

Ag(1)-N(11A)	2.242(13)	Ag(4)-N(11C)	2.228(13)
Ag(1)-N(11B)	2.269(13)	Ag(4)-N(11D)	2.266(13)
Ag(1)-N(22B)	2.362(11)	Ag(4)-N(22C)	2.382(11)
Ag(1)-N(22A)	2.457(10)	Ag(4)-N(22D)	2.449(11)
Ag(2)-N(57B)	2.208(12)	Ag(5)-N(57C)	2.195(12)
Ag(2)-N(42A)	2.255(12)	Ag(5)-N(31D)	2.234(12)
Ag(2)-N(31A)	2.268(12)	Ag(5)-N(42D)	2.330(12)
Ag(3)-N(57A)	2.168(12)	Ag(6)-N(57D)	2.221(12)
Ag(3)-N(31B)	2.256(12)	Ag(6)-N(31C)	2.278(12)
Ag(3)-N(42B)	2.360(13)	Ag(6)-N(42C)	2.315(12)
N(11A)-Ag(1)-N(11B)	158.0(4)	N(11C)-Ag(4)-N(11D)	155.7(4)
N(11A)-Ag(1)-N(22B)	123.4(4)	N(11C)-Ag(4)-N(22C)	73.0(4)
N(11B)-Ag(1)-N(22B)	72.7(4)	N(11D)-Ag(4)-N(22C)	125.7(4)
N(11A)-Ag(1)-N(22A)	71.2(4)	N(11C)-Ag(4)-N(22D)	122.8(4)
N(11B)-Ag(1)-N(22A)	123.4(4)	N(11D)-Ag(4)-N(22D)	72.3(4)
N(22B)-Ag(1)-N(22A)	101.5(4)	N(22C)-Ag(4)-N(22D)	101.8(4)
N(57B)-Ag(2)-N(42A)	128.1(4)	N(57C)-Ag(5)-N(31D)	159.2(4)
N(57B)-Ag(2)-N(31A)	157.3(4)	N(57C)-Ag(5)-N(42D)	126.9(4)
N(42A)-Ag(2)-N(31A)	74.2(4)	N(31D)-Ag(5)-N(42D)	73.7(4)
N(57A)-Ag(3)-N(31B)	160.8(4)	N(57D)-Ag(6)-N(31C)	158.3(4)
N(57A)-Ag(3)-N(42B)	125.8(4)	N(57D)-Ag(6)-N(42C)	128.4(4)
N(31B)-Ag(3)-N(42B)	72.9(4)	N(31C)-Ag(6)-N(42C)	72.5(4)

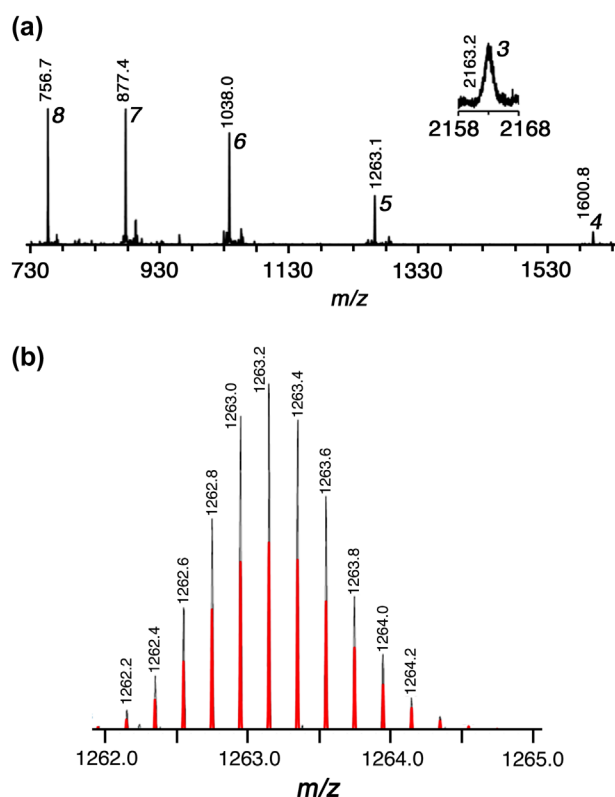


Figure 4. (colour online) (a) Part of the ES mass spectrum of $[\text{Co}_8(\text{L}^{\text{an}})_{12}][\text{BF}_4]_{16}$ showing the sequence of peaks $\{[\text{Co}_8(\text{L}^{\text{an}})_{12}][\text{BF}_4]_{16-n}\}^{n+}$ ($n = 3-8$), arising from loss of tetrafluoroborate anions from the complex. The value of n is shown for each peak along with its m/z value. (b) High-resolution expansion of the signal corresponding to $n = 5$ confirming the charge on the species (red = calculated; black = experimental).

The result from the point of view of the metal ions is that Ag(1) is four-coordinate from two pyrazolyl-pyridine chelates, although it is far from tetrahedral [e.g. the angle N(11A)-Ag(1)-N(11B) is 158°] and the Ag-N separations in the range 2.24–2.46 Å. Ag(2) and Ag(3) in contrast are three-coordinate and virtually planar, with a relatively short bond to the amine donor [2.21/2.17 Å at Ag(2) and Ag(3) respectively] and slightly longer ones to the heterocyclic ligands (2.26 – 2.36 Å). Ag(2) is involved in an additional weak pseudo-axial interaction to a perchlorate ion, with the separation Ag(2)⋯O(61) being 2.77 Å [the closest comparable interaction involving Ag(3) is 2.99 Å]. Overall, the main point here – for the purposes of this work – is that addition of an amine group to the central phenyl spacer fundamentally changes the coordination behaviour of the ligand as the amine becomes involved in metal/ligand coordinate bond formation and the ligand is now pentadentate. The ES mass spectrum confirms that this complex retains its structural integrity in solution: although the most intense signal at m/z 514 arises from the fragment $\{\text{Ag}(\text{L}^{\text{an}})\}^+$, there is also a weak signal at m/z 1337 (value for the most intense component of the isotope

cluster) corresponding to $\{\text{Ag}_3(\text{L}^{\text{an}})_2(\text{ClO}_4)_2\}^+$, i.e. the intact trinuclear complex with loss of one counter-ion.

Reaction of L^{an} with various transition metal dication salts under mild conditions (i.e. MeOH at room temperature or with mild heating) yielded solid products which showed no evidence for formation of a high nuclearity cage. However the more vigorous solvothermal conditions that we usually use for cage preparation, with L^{an} and $\text{Co}(\text{BF}_4)_2$ combined in a 3:2 ratio in methanol and heated to 100 °C for 12 h followed by slow cooling, afforded a crop of small pink crystals which analysed as $[\text{Co}_8(\text{L}^{\text{an}})_{12}][\text{BF}_4]_{16}$ by ESMS: the mass spectrum [Figure 4(a)] displayed a clear series of peaks for the species $\{\text{Co}_8(\text{L}^{\text{an}})_{12}(\text{BF}_4)_{16-n}\}^{n+}$ ($n = 3 - 8$ inclusive), arising by sequential loss of tetrafluoroborate anions from the intact complex cation. High-resolution mass spectrometry analysis confirmed the charge spacings of these peaks; an expansion of the 5 + peak is shown in Figure 4(b) and confirms the charge assignment due to the 0.2 unit spacing on the m/z axis. Also present in the ES mass spectrum were much weaker signals corresponding

to formation of a $\{\text{Co}_6(\text{L}^{\text{an}})_9(\text{BF}_4)_{12-n}\}^{n+}$ species; examples of this type of structure have been structurally characterised previously (17).

The crystals obtained directly from the solvothermal synthesis were not suitable for studying by X-ray diffraction. A ^1H NMR spectrum (Figure 5) is however informative, revealing a dominant set of signals consistent with the presence of two independent ligand environments, with each ligand having no internal symmetry, affording 42 independent ^1H NMR signals spread out over a range of ca. 200 ppm because of the paramagnetism of the Co(II) ions (12,13,22). This number of signals is what would be expected if the $[\text{Co}_8(\text{L}^{\text{an}})_{12}][\text{BF}_4]_{16}$ cage has the S_6 -symmetric structure that has been observed for other $[\text{Co}_8\text{L}_{12}]^{16+}$ cages containing $\text{L}^{\text{m-Ph}}$ and $\text{L}^{2,6\text{-Py}}$, arising from a combination of two *fac* and six *mer* tris-chelate metal centres in a centrosymmetric cage (17–20). We can see particularly clearly in the region between -70 and -110 ppm the presence of four similar signals, which arise from one specific methylene proton occurring in

Table 2. Summary of crystallographic data for the three crystal structures.

Compound	$\text{L}^{\text{an}} \cdot 2.25\text{H}_2\text{O}$	$[\text{Ag}_3(\text{L}^{\text{an}})_2](\text{ClO}_4)_3 \cdot$	$[\text{Co}_8(\text{L}^{\text{an}})_{12}\text{Na}][\text{BF}_4]_{17} \cdot$
		EtOAc·MeNO ₂	4H ₂ O·4MeNO ₂ ·thf
Formula	$\text{C}_{24}\text{H}_{25.3}\text{N}_7\text{O}_{2.25}$	$\text{C}_{53}\text{H}_{53}\text{Ag}_3\text{Cl}_3\text{N}_{15}\text{O}_{16}$	$\text{C}_{296}\text{H}_{280}\text{B}_{17}\text{Co}_8\text{F}_{68}\text{N}_{88}\text{NaO}_{13}$
Molecular weight	448.01	1586.06	7248.26
T/K	100(2)	100(2)	100(2)
Crystal system	Monoclinic	Monoclinic	Tetragonal
Space group	$P2_1/n$	$P2_1/n$	$I4_1/acd$
$a/\text{Å}$	11.4574(3)	15.5708(4)	43.2777(5)
$b/\text{Å}$	10.1888(3)	16.3984(5)	43.2777(5)
$c/\text{Å}$	19.1554(5)	46.2451(13)	39.1423(5)
$\alpha/^\circ$	90	90	90
$\beta/^\circ$	95.3053(12)	98.106(2)	90
$\gamma/^\circ$	90	90	90
$V/\text{Å}^3$	2226.57(11)	11,690.1(6)	73,311.9(19)
Z	4	8	8
$\rho/\text{g cm}^{-3}$	1.336	1.802	1.313
μ/mm^{-1}	0.090	1.216	0.453
Data, restraints, parameters, R_{int}	5183/0/315/0.0249	17,078/1172/1627/0.0625	8564/764/841/0.1075
Final $R1$, $wR2^a$	0.0485, 0.1368	0.1027, 0.3058	0.1580, 0.5658

^aThe value of $R1$ is based on 'observed' data with $I > 2\sigma(I)$; the value of $wR2$ is based on all data.

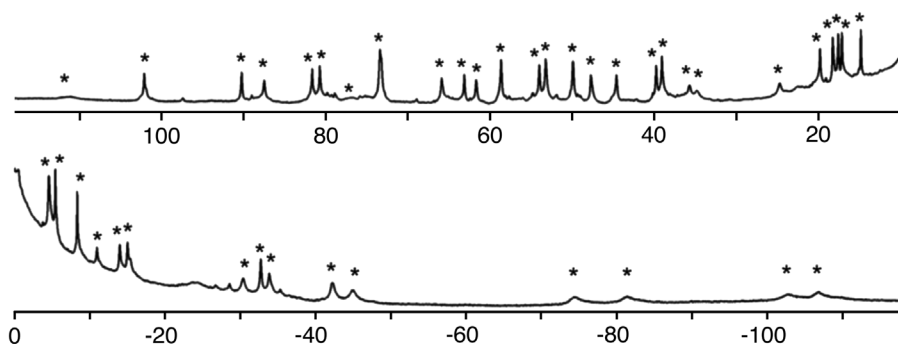


Figure 5. ^1H NMR spectrum (in CD_3NO_2) of redissolved crystals of $[\text{Co}_8(\text{L}^{\text{an}})_{12}][\text{BF}_4]_{16}$ as isolated from the solvothermal synthesis.

Note: Asterisks denote the dominant set of signals which is consistent with the major species in solution being an S_6 -symmetric cage structure with two independent ligand environments.

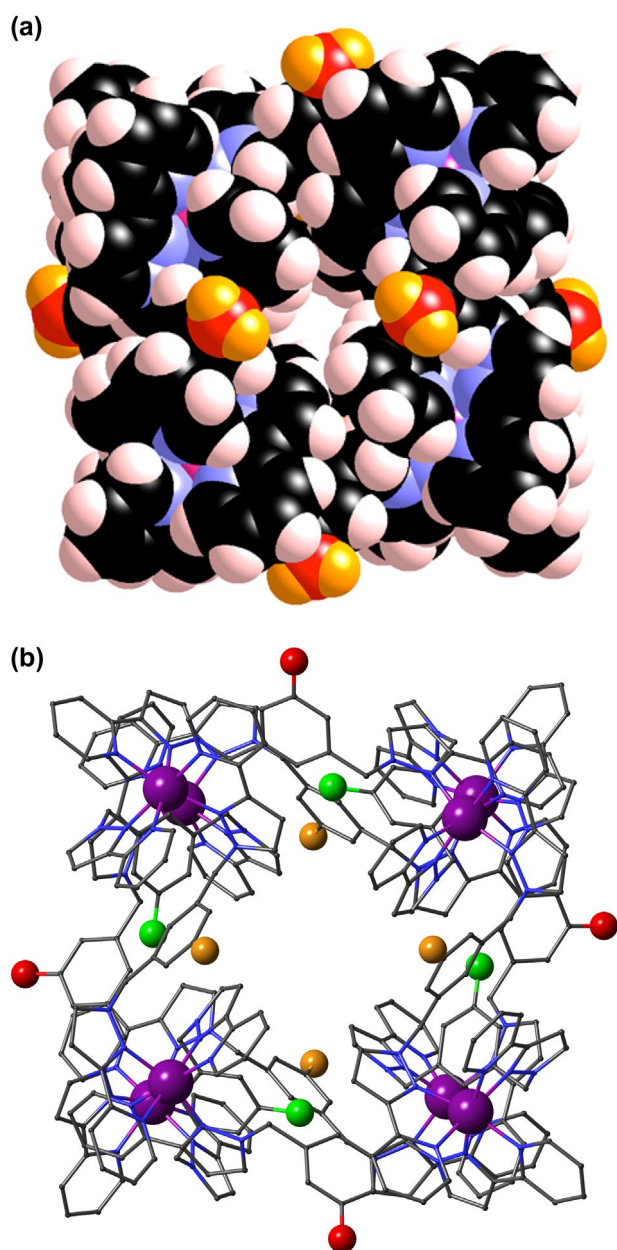


Figure 6. (colour online) Two views of the structure of the cage complex cation of $[\text{Co}_8(\text{L}^{\text{an}})_{12}\text{Na}][\text{BF}_4]_{17}$. (a) Space-filling view, with ligand heterocyclic N atoms in blue and the exterior pendant amine N atoms in red; (b) a view with the ligands in wireframe in which the three sets of crystallographically independent amine groups are shown as coloured spheres (red, green, orange).

four slightly different environments in the cage, as the S_6 symmetry requires (22). The ^1H NMR spectrum is not completely clean, with numerous minor signals also present, suggesting that a material with a different structure is also present (possibly the Co_6L_9 species detected by ESMS, see above). We have observed before that different assemblies can form from the same metal/ligand combination and these can sometimes interconvert slowly in solution; this appears to be an additional example (17,23). The number of signals in the ^1H NMR spectrum of the

major component, however, is clearly consistent with formation of an S_6 -symmetric cube with two independent ligand environments.

Slow diffusion (1–2 months) of tetrahydrofuran vapour into a solution of $[\text{Co}_8(\text{L}^{\text{an}})_{12}][\text{BF}_4]_{16}$ in nitromethane in a glass vial yielded a small crop of crystals of a different habit from the originals and which diffracted better: the crystal structure proved to be of $[\text{Co}_8(\text{L}^{\text{an}})_{12}\text{Na}][\text{BF}_4]_{17}$ (Figure 6). The structure is, as expected, that of an approximately cubic coordination cage, with a pseudo-octahedral metal ion at each vertex coordinated by three pyrazolyl-pyridine chelating units, and a bridging ligand spanning each of the twelve edges. The central amine groups of L^{an} are not involved in coordinate bond formation to the $\text{Co}(\text{II})$ ions [in contrast to what was observed in the $\text{Ag}(\text{I})$ complex, above].

There are two unusual features of this structure compared to other cubic cages formed with $\text{L}^{\text{m-Ph}}$ and $\text{L}^{2,6\text{-Py}}$ (17–20). Firstly, it does not have the usual S_6 -symmetric structure. Instead, there are four *fac* tris-chelate metal complex vertices and four *mer* tris-chelate vertices which alternate around the cube, meaning that the assembly as a whole has S_4 symmetry with three crystallographically independent ligand environments rather than two. Secondly, the cavity contains at its centre a Na^+ cation which is coordinated by four $[\text{BF}_4]^-$ anions; effectively the cavity contains a $\{\text{Na}(\text{BF}_4)_4\}^{3-}$ complex anion as the guest (Figures 6 and 7). We assume that the Na^+ cation has arisen from prolonged exposure of the complex to glass during the crystallisation process, which explains why the crystals took months to grow. We have observed this type of structure once before (24).

The positioning of the peripheral amine groups is significant as four of them lie along the cage surface and become involved in weak interactions with the cage contents through the portals, whereas the other ones are externally-directed. In accord with the molecular symmetry the twelve pendant amine groups are not all crystallographically equivalent but split into three sets of four [N(61A), N(61B), N(61C)] which are labelled in different colours in Figure 6(b) which looks along the cage S_4 axis. The four N(61C) amine groups, shown in green in Figure 6(b), are positioned so that they block the windows of four of the six faces of the cube in an equatorial ‘belt’ with the C–N bonds lying along the cube faces. The remaining two faces, on opposite sides of the cage, are not blocked by amines, but are each flanked by two amine groups N(61A) (orange in Figure 6(b)) which are outwardly directed away from the cage core. Finally the four amines N(61B) (red in Figure 6(b)) are also externally directed.

The $\{\text{Na}(\text{BF}_4)_4\}^{3-}$ complex guest interacts with the cage surface in two ways. It is involved in $\text{CH}\cdots\text{F}$ hydrogen

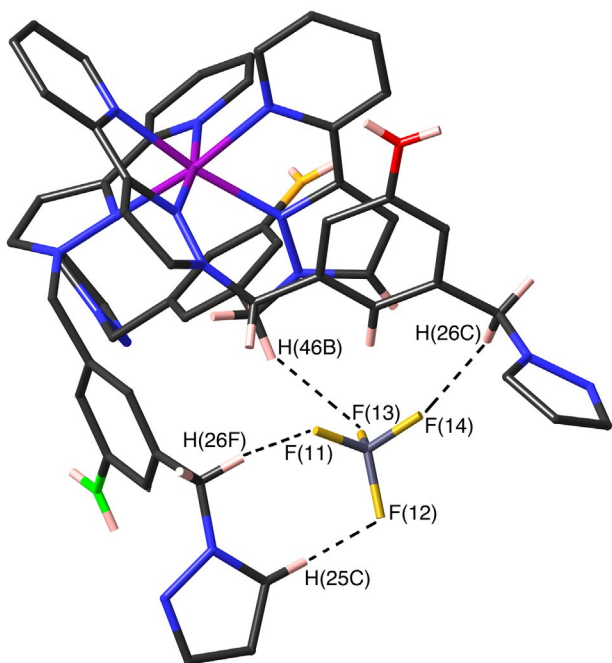


Figure 7. (colour online) One of the *fac* tris-chelate Co(II) vertices in the structure of $[\text{Co}_8(\text{L}^{\text{an}})_{12}\text{Na}][\text{BF}_4]_{17}$ showing CH...F interactions with the nearby fluoroborate anion: dashed lines indicate H...F separations of $< 2.5 \text{ \AA}$ (sum of van der Waals radii is 2.67 \AA).

bonds with inwardly-directed CH protons lining the interior of the cage surface (Figure 7), particularly at the *fac* tris-chelate vertices which form good H-bond donor pockets due to the high electrostatic charge potential close to the Co(II) ions (25,26). In addition, the complex anion guest forms multiple NH...F hydrogen bonds with the four amine groups on the cage surface that lie above the portals (Figure 8). Specifically, each amine group N(61C) is involved in three short N...F contacts (distances 3.49, 3.65 and 3.66 Å; see Figure 8(b)) with one of the four tetrafluoroborate anions, indicative of a trifurcated NH...anion contact. The reason that four of the twelve amine groups on the cage exterior lie around the surface close to cage portals is now clear: each of these interacts with one of the four tetrafluoroborate anions inside the cavity, with the interaction between external amine group and internal anion occurring through the cage windows. The guest anions are disposed such that they present their externally-facing F atoms to the 'belt' of four equatorial portals in the cage where the amines lie; the guest anions lie further away from the other two cage portals, and the amine groups close to those are therefore directed outwards to participate in H-bonding interactions with solvent molecules or anions *outside* the cages. This interaction of exohedral functional groups with the contents of the cavity inside the cage is unusual and clearly plays a significant role in the host-guest chemistry of the cage in a way that was not expected.

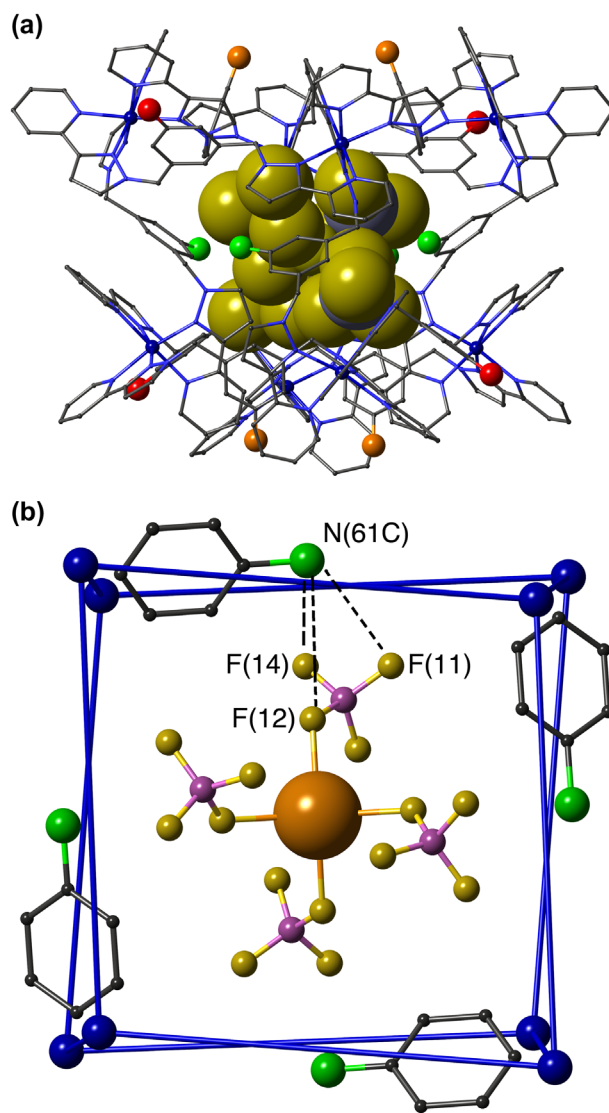


Figure 8. (colour online) Two additional views of the structure of the complex cation of $[\text{Co}_8(\text{L}^{\text{an}})_{12}\text{Na}][\text{BF}_4]_{17}$ emphasising the cavity contents and their interaction with the peripheral amine groups. (a) A view of the cage in wireframe with the contents of the cavity in space-filling view, showing the close contact with the four amines N(61C) (shown in green) around the 'belt'; (b) a view illustrating the trifurcated NH...F interactions involving the guest cluster and the N(61C) amine NH_2 groups [non-bonded N(61C)...F separations: 3.49, 3.66 and 3.65 Å to F(11), F(14) and F(12) respectively].

This S_4 -symmetric structure is clearly inconsistent with the ^1H NMR spectrum in Figure 5, as the presence of three independent ligand environments with no internal symmetry would generate 63 ^1H signals; the region between -70 and -110 ppm, for example, would contain six signals and not four. The S_4 symmetric cage structure that is observed in the solid state is clearly a better symmetry match for the guest complex $\{\text{Na}(\text{BF}_4)_4\}^{3-}$ than the S_6 symmetric cage would be, as it provides an array of H-bonding interactions complementary to the guest (Figures 7 and 8)

which could therefore stabilise/template the S_4 -symmetric host. We suggest therefore that the initially formed S_6 symmetric cage slowly rearranges to the S_4 -symmetric version on crystallisation to accommodate and complement the $\{\text{Na}(\text{BF}_4)_4\}^{3-}$ anion. We note that the variation of individual metal centres between *fac* and *mer* tris-chelate coordination geometry in cage superstructures has been highlighted by others (27), and provides additional (and often unexpected) structural complexity. The general area of supramolecular transformations within self-assembled metal/ligand architectures is of considerable topical interest and has recently been reviewed (28).

Unfortunately we were unable to obtain a ^1H NMR spectrum of redissolved crystals of $[\text{Co}_8(\text{L}^{\text{an}})_{12}\text{Na}][\text{BF}_4]_{17}$ as these crystals only formed in very small amounts (even in the presence of excess NaBF_4) and had poor solubility. It is likely however that polar solvents would break the hydrogen-bonding interactions around the guest complex $\{\text{Na}(\text{BF}_4)_4\}^{3-}$, resulting in solvation of the Na^+ cation and fluoroborate anions.

Conclusion

We prepared the new ligand L^{an} as an amine-functionalised analogue of $\text{L}^{\text{m-Ph}}$ which might allow access to externally-functionalised cages; that possibility remains. Initial studies of its coordination behaviour show some interesting behaviour. Firstly, the amine group can alter the coordination behaviour of the ligand, which is pentadentate instead of tetradentate in an unusual double-helical trinuclear complex with $\text{Ag}(\text{I})$. Secondly, and in contrast to this, the amine groups on L^{an} do not interfere with formation of a cage structure in the form of the approximately cubic assembly $[\text{Co}_8(\text{L}^{\text{an}})_{12}][\text{BF}_4]_{16}$ (based on mass spectrometric and NMR evidence) but become involved in hydrogen-bonding interactions with the complex anion guest $\{\text{Na}(\text{BF}_4)_4\}^{3-}$. Thus the exterior amine groups form $\text{NH}\cdots\text{F}$ interactions with the internal guest, through the portals in the cage surface; the cage structure undergoes significant rearrangement from S_6 to S_4 symmetry to allow binding of the fourfold symmetric guest.

Experimental section

General details

3-(2-Pyridyl)pyrazole was prepared as reported previously (29). Instrumentation used for routine NMR and mass spectrometric analysis has been reported in recent publications (23–25). Compounds **1** (15), **2** (16) and **3** (16) were prepared according to the literature methods. The perchlorate complex included in this work was prepared in small amounts and was stable for routine synthesis and

purification procedures. However, caution should be exercised because perchlorate salts of metal complexes with organic ligands are potentially explosive.

Syntheses

Compound 4

A mixture of **3** (1.88 g, 5.0 mmol), 3-(2-pyridyl)pyrazole (1.54 g, 10.6 mmol), THF (50 cm^3) and aqueous NaOH (17.5 M, 6 cm^3) was stirred at 75 °C for 3 days. The organic layer was separated, dried over MgSO_4 and concentrated before purification by silica column. Elution with $\text{EtOAc}/\text{CH}_2\text{Cl}_2$ (4:1) \rightarrow 100% EtOAc yielded two fractions. The first fraction collected yielded **4** as an off-white solid (Yield: 1.78 g, 3.5 mmol, 70%), and the second fraction yielded the Boc-protected L^{an} as an off-white solid (yield: 0.41 g, 1.0 mmol, 20%; total yield 90%). ^1H -NMR (400 MHz, CDCl_3): δ 8.57 (2H, ddd; pyridyl H^6), 7.87 (2H, dt; pyridyl H^3), 7.63 (2H, td; pyridyl H^4), 7.37 (1H, s; ArH), 7.35 (2H, d; pyrazolyl H^5), 7.20 (2H, s; ArH), 7.14 (2H, ddd; pyridyl H^5), 6.84 (2H, d; pyrazolyl H^4), 6.71 (1H, bs; NH), 5.22 (4H, s; CH_2), 1.41 (9H, s; ^tBu). ESMS: m/z 530 $[\text{M} + \text{Na}]^+$, 508 $[\text{M} + \text{H}]^+$, 452 $[\text{M} - ^t\text{Bu} + 2\text{H}]^+$, 255 $[\text{M} + 2\text{H}]^{2+}$, 227 $[\text{M} - ^t\text{Bu} + 3\text{H}]^{2+}$.

L^{an}

To a solution of **4** (1.78 g, 3.5 mmol) in CH_2Cl_2 (10 cm^3) was added TFA (10 cm^3) and the resultant clear yellow solution was stirred at 25 °C for 14 h. The solvent was removed *in vacuo* and the clear brown oil was repeatedly washed with $\text{CH}_2\text{Cl}_2/\text{MeOH}$ (1:1) and evaporated to dryness in order to remove all traces of TFA. The brown solid was washed with aqueous K_2CO_3 and the organic layer extracted with CH_2Cl_2 , dried over MgSO_4 and evaporated to dryness, yielding L^{an} as a white solid (Yield: 1.13 g, 79%). X-ray quality crystals were grown by slow evaporation of a solution of L^{an} in ethyl acetate and hexane. ^1H -NMR (400 MHz, CDCl_3): δ 8.62 (2H, ddd; pyridyl H^6), 7.92 (2H, dt; pyridyl H^3), 7.68 (2H, td; pyridyl H^4), 7.39 (2H, d; pyrazolyl H^5), 7.18 (2H, ddd; pyridyl H^5), 6.89 (2H, d; pyrazolyl H^4), 6.51 (1H, s; ArH), 6.39 (2H, s; ArH), 5.23 (4H, s; CH_2), 3.64 (2H, bs; NH_2). ESMS: m/z 430 $[\text{M} + \text{Na}]^+$, 408 $[\text{M} + \text{H}]^+$, 205 $[\text{M} + 2\text{H}]^{2+}$. Found: C, 64.40; H, 5.53; N, 21.92%. Required for $\text{C}_{24}\text{H}_{21}\text{N}_7 \cdot 2.25\text{H}_2\text{O}$: C, 64.34; H, 5.74; N, 21.89%.

$[\text{Co}_8(\text{L}^{\text{an}})_{12}][\text{BF}_4]_{16}$

A Teflon lined autoclave was charged with L^{an} (0.050 g, 0.12 mmol), $\text{Co}(\text{BF}_4)_2 \cdot 6\text{H}_2\text{O}$ (0.036 g, 0.10 mmol) and methanol (5 cm^3). Heating to 100 °C for 12 h followed by slow cooling to room temperature yielded a crop of small pink crystals, which were washed with methanol and dried to give $[\text{Co}_8(\text{L}^{\text{an}})_{12}][\text{BF}_4]_{16}$ as a pink solid in 76% yield. ESMS:

m/z ; 2163.2, $\{[\text{Co}_8(\text{L}^{\text{an}})_{12}](\text{BF}_4)_{13}\}^{3+}$; 1600.8, $\{[\text{Co}_8(\text{L}^{\text{an}})_{12}](\text{BF}_4)_{12}\}^{4+}$; 1263.1, $\{[\text{Co}_8(\text{L}^{\text{an}})_{12}](\text{BF}_4)_{11}\}^{5+}$, 1038.0 $\{[\text{Co}_8(\text{L}^{\text{an}})_{12}](\text{BF}_4)_{10}\}^{6+}$; 877.4, $\{[\text{Co}_8(\text{L}^{\text{an}})_{12}](\text{BF}_4)_9\}^{7+}$; 756.7, $\{[\text{Co}_8(\text{L}^{\text{an}})_{12}](\text{BF}_4)_8\}^{8+}$. Elemental analytical data was consistent with the presence of water of crystallisation due to the desolvated material being hygroscopic. Found: C, 47.52; H, 4.17; N, 15.76%. Required for $\text{C}_{288}\text{H}_{252}\text{B}_{16}\text{Co}_8\text{F}_{64}\text{N}_{84}\cdot 32\text{H}_2\text{O}$: C, 47.21; H, 4.35; N, 16.06%. Note that we have recently structurally characterised a similar cage complex containing 28 water molecules per formula unit so the value of 32 here which gives the optimal fit for elemental analytical data is not unreasonable (30).

$[\text{Ag}_3(\text{L}^{\text{an}})_2](\text{ClO}_4)_3$

A mixture of L^{an} (0.050 g, 0.12 mmol) and $\text{Ag}(\text{ClO}_4)$ (0.040 g, 0.16 mmol), methanol (5 cm³) and DCM (5 cm³) was stirred at room temperature overnight. The resultant precipitate was collected by filtration off and washed with methanol and DCM, and then dried *in vacuo* to give $[\text{Ag}_3(\text{L}^{\text{an}})_2](\text{ClO}_4)_3$ as a grey powder in 65% yield. ¹H-NMR (250 MHz, CD₃CN): δ 8.32 (1H, d), 8.11–7.88 (6H, m), 7.84 (1H, d), 7.48 (3H, m), 6.98 (3H, m), 6.56 (1H, s), 5.14 (3H, m), 4.30 (1H, d). ESMS: m/z 514, $\{\text{Ag}(\text{L}^{\text{an}})\}^+$; 1337, $\{\text{Ag}_3(\text{L}^{\text{an}})_2(\text{ClO}_4)_2\}^+$ (correct isotopic pattern was observed).

X-ray crystallography

Details of the crystal, data collection and refinement parameters are summarised in Table 2. Diffraction data for the structures $\text{L}^{\text{an}}\cdot 2.25\text{H}_2\text{O}$ and $[\text{Ag}_3(\text{L}^{\text{an}})_2](\text{ClO}_4)_3\cdot \text{EtOAc}\cdot \text{MeNO}_2$ were collected on a Bruker Apex-II diffractometer at the University of Sheffield. Diffraction data for $[\text{Co}_8(\text{L}^{\text{an}})_{12}\text{Na}][\text{BF}_4]_{17}\cdot 4\text{H}_2\text{O}\cdot 4\text{MeNO}_2\cdot \text{thf}$ were collected by the EPSRC National Crystallography Service using a synchrotron radiation source (31). Data were corrected for absorption using empirical methods (SADABS) based upon symmetry-equivalent reflections combined with measurements at different azimuthal angles (32). The structures were solved by direct methods and refined by full-matrix least squares on weighted F^2 values for all reflections using the SHELX suite of programs (33). Non-hydrogen atoms were refined anisotropically. Hydrogen atoms were placed in calculated positions, refined using idealized geometries (riding model) and were assigned fixed isotropic displacement parameters.

The crystals of $[\text{Co}_8(\text{L}^{\text{an}})_{12}\text{Na}](\text{BF}_4)_{17}$ exhibited weak scattering due to a combination of poor crystallinity, solvation, and disorder of anions/solvent molecules. The structure and connectivity of the complex cation could however be unambiguously determined with reasonable precision. Extensive use of geometric restraints on aromatic rings and anions, and restraints on aromatic displacement parameters, were required to keep refinement stable.

Solvent molecules that could be modelled satisfactorily were included in the final refinements; large regions of diffuse electron density that could not be modelled (from disordered solvents/counter-ions) were removed from the refinement, using the SQUEEZE function in PLATON (34). Full details are in the CIF. CCDC deposition numbers: 1564119–1564121.

Acknowledgements

We thank Mr. Harry Adams for assistance with the crystallography, and the EPSRC for financial support [grant EP/N031555].

Disclosure statement

No potential conflict of interest was reported by the authors.

Funding

This work was supported by the Engineering and Physical Sciences Research Council (EPSRC) [EP/N031555].

ORCID

Alexander J. Metherell  <http://orcid.org/0000-0003-0672-7940>

Michael D. Ward  <http://orcid.org/0000-0001-8175-8822>

References

- (1) (a) Cook, T.R.; Stang, P.J. *Chem. Rev.* **2015**, *115*, 7001–7045. (b) Breiner, B.; Clegg, J.K.; Nitschke, J.R. *Chem. Sci.* **2011**, *2*, 51–56. (c) Yoshizawa, M.; Klosterman, J.K.; Fujita, M. *Angew. Chem. Int. Ed.* **2009**, *48*, 3418–3438. (d) Ward, M.D.; Hunter, C.A.; Williams, N.H. *Chem. Lett.* **2017**, *46*, 2–9. (e) Pluth, M.D.; Bergman, R.G.; Raymond, K.N. *Acc. Chem. Res.* **2009**, *42*, 1650–1659. (f) Vardhan, H.; Yusubov, M.; Verpoort, F. *Coord. Chem. Rev.* **2016**, *306*, 171–194. (g) Han, M.; Engelhard, D.M.; Clever, G.H. *Chem. Soc. Rev.* **2014**, *43*, 1848–1860. (h) Amouri, H.; Desmarests, C.; Moussa, J. *Chem. Rev.* **2014**, *112*, 2015–2041. (i) Chen, L.-J.; Yang, H.-B.; Shionoya, M. *Chem. Soc. Rev.* **2017**, *46*, 2555–2576.
- (2) Ward, M.D.; Raithby, P.R. *Chem. Soc. Rev.* **2013**, *42*, 1619–1636.
- (3) (a) Lewis, J.E.M.; Gavey, E.L.; Cameron, S.A.; Crowley, J.D. *Chem. Sci.* **2012**, *3*, 778–784. (b) Yi, J.W.; Barry, N.P.E.; Furrer, M.A.; Zava, O.; Dyson, P.J.; Therrien, B.; Kim, B.H. *Bioconjugate Chem.* **2012**, *23*, 461–471. (c) Mal, P.; Schultz, D.; Beyeh, K.; Rissanen, K.; Nitschke, J.R. *Angew. Chem., Int. Ed.* **2008**, *47*, 8297–8301.
- (4) Harris, K.; Fujita, D.; Fujita, M. *Chem. Commun.* **2013**, *49*, 6703–6712.
- (5) Kamiya, N.; Tominaga, M.; Sato, S.; Fujita, M. *J. Am. Chem. Soc.* **2007**, *129*, 3816–3817.
- (6) Tominaga, M.; Suzuki, K.; Murase, T.; Fujita, M. *J. Am. Chem. Soc.* **2005**, *127*, 11950–11951.
- (7) Suzuki, K.; Sato, S.; Fujita, M. *Nature Chem.* **2010**, *2*, 25–29.
- (8) Neelakandan, P.P.; Jimenez, A.; Nitschke, J.R. *Chem. Sci.* **2014**, *5*, 908–915.

- (9) Custelcean, R.; Bosano, L.; Bonnesen, P.V.; Kertesz, V.; Hay, B.P. *Angew. Chem. Int. Ed.* **2009**, *48*, 4025–4029.
- (10) Desmarets, C.; Gontard, G.; Cooksy, A.L.; Rager, M.N.; Amouri, H. *Inorg. Chem.* **2014**, *53*, 4287–4294.
- (11) Elliott, A.B.S.; Lewis, J.E.M.; van der Salm, H.; McAdam, C.J.; Crowley, J.D.; Gordon, K.C. *Inorg. Chem.* **2016**, *55*, 3440–3447.
- (12) Whitehead, M.; Turega, S.; Stephenson, A.; Hunter, C.A.; Ward, M.D. *Chem. Sci.* **2013**, *4*, 2744–2751.
- (13) (a) Cullen, W.; Misuraca, M.C.; Hunter, C.A.; Williams, N.H.; Ward, M.D. *Nature Chem.* **2016**, *8*, 231–236. (b) Cullen, W.; Turega, S.; Hunter, C.A.; Ward, M.D. *Chem. Sci.* **2015**, *6*, 625–631. (c) Turega, S.; Cullen, W.; Whitehead, M.; Hunter, C.A.; Ward, M.D. *J. Am. Chem. Soc.* **2014**, *136*, 8475–8483.
- (14) Metherell, A.J.; Ward, M.D. *RSC Adv.* **2013**, *3*, 14281–14285.
- (15) Neelapapu, R.; Holzle, D.L.; Velaparthi, S.; Bai, H.; Brunsteiner, M.; Blond, S.Y.; Petukhov, P.A. *J. Med. Chem.* **2011**, *54*, 4350–4364.
- (16) Onagi, H.; Rebek, J. *Chem. Commun.* **2005**, 4604–4606.
- (17) Najar, A.M.; Tidmarsh, I.S.; Adams, S.; Ward, M.D. *Inorg. Chem.* **2009**, *48*, 11871–11881.
- (18) Stephenson, A.; Ward, M.D. *Dalton Trans.* **2011**, *40*, 10360–10369.
- (19) Bell, Z.R.; Harding, L.P.; Ward, M.D. *Chem. Commun.* **2003**, 2432–2433.
- (20) Argent, S.P.; Adams, H.; Harding, L.P.; Ward, M.D. *Dalton Trans.* **2006**, 542–544.
- (21) Stephenson, A.; Ward, M.D. *RSC Adv.* **2012**, *2*, 10844–10853.
- (22) Tidmarsh, I.S.; Taylor, B.F.; Hardie, M.J.; Russo, L.; Clegg, W.; Ward, M.D. *New J. Chem.* **2009**, *33*, 366–375.
- (23) (a) Stephenson, A.; Argent, S.P.; Riis-Johannessen, T.; Tidmarsh, I.S.; Ward, M.D. *J. Am. Chem. Soc.* **2011**, *133*, 858–870. (b) Cullen, W.; Hunter, C.A.; Ward, M.D. *Inorg. Chem.* **2015**, *54*, 2626–2637.
- (24) Metherell, A.J.; Ward, M.D. *RSC Adv.* **2016**, *6*, 10750–10762.
- (25) Turega, S.; Whitehead, M.; Hall, B.R.; Meijer, A.J.H.M.; Hunter, C.A.; Ward, M.D. *Inorg. Chem.* **2013**, *52*, 1122–1132.
- (26) Metherell, A.J.; Ward, M.D. *Dalton Trans.* **2016**, *45*, 16096–16111.
- (27) (a) Hall, B.R.; Adams, H.; Ward, M.D. *Supramol. Chem.* **2012**, *24*, 499–507. (b) Beissel, T.; Powers, R.E.; Parac, T.N.; Raymond, K.N. *J. Am. Chem. Soc.* **1999**, *121*, 4200–4206. (c) Meng, W.; Clegg, J.K.; Thoburn, J.D.; Nitschke, J.R. *J. Am. Chem. Soc.* **2011**, *133*, 13652–13660. (d) Kieffer, M.; Pilgrim, B.S.; Ronson, T.K.; Roberts, D.A.; Aleksanyan, M.; Nitschke, J.R. *J. Am. Chem. Soc.* **2016**, *138*, 6813–6821.
- (28) Wang, W.; Wang, Y.-X.; Yang, H.-B. *Chem. Soc. Rev.* **2016**, *45*, 2656–2693.
- (29) Amoroso, A.J.; Cargill Thompson, A.M.W.; Jeffery, J.C.; Jones, P.L.; McCleverty, J.A.; Ward, M.D. *Chem. Commun.* **1994**, 2751–2752.
- (30) Metherell, A. J.; Cullen, W.; Williams, N. H.; Ward, M. D. *submitted for publication*.
- (31) Coles, S.J.; Gale, P.A. *Chem. Sci.* **2012**, *3*, 683–689.
- (32) Sheldrick, G.M. *SADABS: A program for absorption correction with the Siemens SMART system*; University of Göttingen, Germany, **1996**.
- (33) Sheldrick, G.M. *Acta Cryst. A* **2008**, *64*, 112–122.
- (34) Vandersluis, P.; Spek, A.L. *Acta Cryst. A* **1990**, *46*, 194–201.